J|A|C|S ARTICLES

Published on Web 07/10/2009

"Breathing" Vesicles

Shaoyong Yu,[†] Tony Azzam,[†] Isabelle Rouiller,[‡] and Adi Eisenberg*[,†]

Department of Chemistry, McGill University, 801 Sherbrooke Street West, Montreal, Quebec, H3A 2K6, Canada, and Department of Anatomy and Cell Biology, McGill University, 3640 University Street, Montreal, Quebec, H3A 2B2, Canada

Received April 9, 2009; E-mail: adi.eisenberg@mcgill.ca

Abstract: A vesicle system is described that possesses a pH-induced "breathing" feature and consists of a three-layered wall structure. The "breathing" feature consists of a highly reversible vesicle volume change by a factor of ca. 7, accompanied by diffusion of species into and out of the vesicles with a relaxation time of ca. 1 min. The triblock copolymer poly(ethylene oxide)$_{45}$-*block*-polystyrene$_{130}$-*block*-poly(2-diethylaminoethyl methacrylate)$_{120}$ (PEO_{45}-b-PS_{130}-b-$PDEA_{120}$) was synthesized via ATRP. Self-assembly into vesicles was carried out at a pH of ca.10.4. The vesicle wall was shown by cryo-TEM to consist of a sandwich of two external ca. 4 nm thick continuous PS layers and one ca. 17 nm thick PDEA layer in the middle. As the pH decreases, both the vesicle size and the thickness of all three layers increase. The increase of the thickness of the intermediate PDEA layer arises from the protonation and hydration, but the swelling is constrained by the PS layers. The increase of the thickness of the two PS layers is a result of an increasing incompatibility and an accompanying sharpening of the interface between the PS layers and the PDEA layer. Starting at a pH slightly below 6, progressive swelling of the PDEA layer with decreasing pH induces a cracking of the two PS layers and also a sharp increase of the vesicle size and the wall thickness. By pH 3.4, the vesicle size has increased by a factor of ~1.9 and the wall shows a cracked surface. These changes between pH 10.4 and 3.4 are highly reversible with the relaxation time of ca. 1 min and can be performed repeatedly. The change in the wall structure not only increases dramatically the wall permeability to water but also greatly expands the rate of proton diffusion from practically zero to extremely rapid.

Introduction

Vesicles prepared from amphiphilic block copolymers are part of a morphological continuum, which includes spheres, rods, vesicles, etc.[1,2] These various morphologies have attracted extensive attention in the past decade, and many reviews have been published.[3−20] Compared to their low molecular counterpart, i.e., the liposomes, polymer vesicles show higher stability and a highly designable permeability[21] and have thus received the attention of many researchers.[22−32] The active research in this field is not unexpected since vesicles could be potentially

[†] Department of Chemistry.
[‡] Department of Anatomy and Cell Biology.

(1) Zhang, L. F.; Eisenberg, A. *Science* **1995**, *268*, 1728–1731.
(2) Zhang, L. F.; Eisenberg, A. *J. Am. Chem. Soc.* **1996**, *118*, 3168–3181.
(3) Rosler, A.; Vandermeulen, G. W. M.; Klok, H. A. *Adv. Drug Delivery Rev.* **2001**, *53*, 95–108.
(4) Zhang, G. Z.; Niu, A. Z.; Peng, S. F.; Jiang, M.; Tu, Y. F.; Li, M.; Wu, C. *Acc. Chem. Res.* **2001**, *34*, 249–256.
(5) Riess, G. *Prog. Polym. Sci.* **2003**, *28*, 1107–1170.
(6) Hamley, I. W. *Nanotechnology* **2003**, *14*, R39–R54.
(7) Ikkala, O.; ten Brinke, G. *Chem. Commun.* **2004**, 2131–2137.
(8) Forster, S.; Abetz, V.; Muller, A. H. E. In *Polyelectrolytes with Defined Molecular Architecture II*; Springer-Verlag: Berlin, 2004; Vol. 166, pp 173−210.
(9) Chen, D. Y.; Jiang, M. *Acc. Chem. Res.* **2005**, *38*, 494–502.
(10) Rodriguez-Hernandez, J.; Checot, F.; Gnanou, Y.; Lecommandoux, S. *Prog. Polym. Sci.* **2005**, *30*, 691–724.
(11) Gohy, J. F. In *Block Copolymers II*; Springer-Verlag: Berlin, 2005; Vol. 190, pp 65−136.
(12) Harada, A.; Kataoka, K. *Prog. Polym. Sci.* **2006**, *31*, 949–982.
(13) O'Reilly, R. K.; Hawker, C. J.; Wooley, K. L. *Chem. Soc. Rev.* **2006**, *35*, 1068–1083.
(14) Liu, G. In *Block Copolymers in Nanoscience*; Lazzari, M., Liu, G., Lecommandoux, S., Eds.; Wiley-VCH: Weinheim, 2006; pp 233−256.
(15) Letchford, K.; Burt, H. *Eur. J. Pharm. Biopharm.* **2007**, *65*, 259–269.
(16) Smart, T.; Lomas, H.; Massignani, M.; Flores-Merino, M. V.; Perez, L. R.; Battaglia, G. *Nano Today* **2008**, *3*, 38–46.
(17) McCormick, C. L.; Sumerlin, B. S.; Lokitz, B. S.; Stempka, J. E. *Soft Matter* **2008**, *4*, 1760–1773.
(18) Zhou, Y.; Yan, D. *Chem. Commun.* **2009**, 1172–1188.
(19) Vriezema, D. M.; Aragones, M. C.; Elemans, J.; Cornelissen, J.; Rowan, A. E.; Nolte, R. J. M. *Chem. Rev.* **2005**, *105*, 1445–1489.
(20) Blanazs, A.; Armes, S. P.; Ryan, A. J. *Macromol. Rapid Commun.* **2009**, *30*, 267–277.
(21) Discher, B. M.; Won, Y. Y.; Ege, D. S.; Lee, J. C. M.; Bates, F. S.; Discher, D. E.; Hammer, D. A. *Science* **1999**, *284*, 1143–1146.
(22) Discher, B. M.; Hammer, D. A.; Bates, F. S.; Discher, D. E. *Curr. Opin. Colloid Interface Sci.* **2000**, *5*, 125–131.
(23) Discher, D. E.; Eisenberg, A. *Science* **2002**, *297*, 967–973.
(24) Antonietti, M.; Forster, S. *Adv. Mater.* **2003**, *15*, 1323–1333.
(25) Bellomo, E. G.; Wyrsta, M. D.; Pakstis, L.; Pochan, D. J.; Deming, T. J. *Nat. Mater.* **2004**, *3*, 244–248.
(26) Kita-Tokarczyk, K.; Grumelard, J.; Haefele, T.; Meier, W. *Polymer* **2005**, *46*, 3540–3563.
(27) Du, J. Z.; Tang, Y. P.; Lewis, A. L.; Armes, S. P. *J. Am. Chem. Soc.* **2005**, *127*, 17982–17983.
(28) Li, Y.; Lokitz, B. S.; McCormick, C. L. *Angew. Chem., Int. Ed.* **2006**, *45*, 5792–5795.
(29) Mecke, A.; Dittrich, C.; Meier, W. *Soft Matter* **2006**, *2*, 751–759.
(30) Davis, K. P.; Lodge, T. P.; Bates, F. S. *Macromolecules* **2008**, *41*, 8289–8291.
(31) Rank, A.; Hauschild, S.; Forster, S.; Schubert, R. *Langmuir* **2009**, *25*, 1337–1344.
(32) Ott, C.; Hoogenboom, R.; Hoeppener, S.; Wouters, D.; Gohy, J. F.; Schubert, U. S. *Soft Matter.* **2009**, *5*, 84–91.

useful in many fields, such as drug delivery,[33−38] nanoreactors,[39−42] biological functional models,[43,44] and others.

Many of these possible applications require control of vesicle sizes; thus this aspect has become one of the important topics in vesicle research. The size of vesicles can be controlled during their formation or can be changed after formation. During vesicle formation, the size can be controlled by employing block polymers with different molecular weights,[45] polydispersity,[46,47] hydrophilic/hydrophobic ratio,[48] or polymer concentration,[49,50] by changing the solvent nature and composition,[51] by tuning solution pH,[52] by use of additives such as ions,[53,54] surfactants,[55] homopolymers,[2] block copolymers,[56] or dendrimers,[57] and by altering other parameters. Changing vesicle size after formation is also possible. The size change mechanism involves the fusion and fission of vesicles, the swelling and shrinkage of the vesicle wall, or the extension or collapse of the corona while keeping the wall diameter constant. Details will be discussed below.

In 1999, Shen and Eisenberg[58] demonstrated a controllable and reversible size change in vesicles prepared from PS_{310}-b-PAA_{52} (the numbers denote the number of repeat units) by changing the water content in dioxane from 28 wt % to 40 wt % and back to 29%. Later, in 2001, Luo and Eisenberg[59] elucidated the size change mechanism as consisting of fusion and fission of vesicles driven by the interfacial energy change in response to varying water contents. In 2003, Choucair and Eisenberg[60] determined the relaxation time of the vesicle fusion and fission processes to be on the order of minutes. Recently, Mai, Zhou, and Yan[61] reported the direct observation of the real-time process from small vesicles fusing into big vesicles in a hyperbranched copolymer system.

Swelling of the vesicle wall by itself can also induce a vesicle size change. In 2005, in a pioneering study, Du and Armes[62] synthesized poly(ethylene oxide)-*block*-poly[2-(diethylamino)-ethyl methacrylate-*stat*-3-(trimethoxysilyl)propyl methacrylate] [PEO-b-P(DEA-*stat*-TMSPMA)] and produced vesicles with a cross-linked TMSPMA component in the wall. The other wall-forming component, PDEA, which is pH-sensitive, allows the vesicle size to change with pH. The maximum volume increase was reported to be 123%.

The extension and collapse of corona chains, realized, for example, by the secondary structure transition of peptides, can also induce vesicle size changes. In 2002, Chécot, Lecommandoux, and Klok[63] reported a pH-sensitive vesicle system prepared from polybutadiene-b-poly(L-glutamic acid) (PB-b-PGA). The vesicles show a reversible size variation from 100 to 160 nm. The authors found that the pH-induced changes correlate with the secondary structure transition of the corona chains with pH. In 2007, Sigel and Schlaad[64] reported the size change of peptide block copolymers polybutadiene-b-poly(L-lysine). They found that the size change was caused by the packing density of chains attributed to changes in the secondary structure and the ionization of corona chains. Gebhardt and Savin[65] further analyzed the contributions from the helix−coil transition and associated charge−charge interactions within the corona chains with regard to a similar vesicle system. More recently, Shi, Zhou, and Yan[66] reported a reversible size change, from 200 nm to a few micrometers, of vesicles prepared from carboxy-terminated hyperbranched polyesters. It was suggested that the deprotonation of corona carboxyl groups lessened the preferred curvature of the vesicles, i.e., led to an increase in the vesicle size. Clearly, vesicles with a pH-sensitive corona will change their size with pH even if the wall size remains constant.

In this paper, we report on a vesicle system with a pH-induced "breathing" feature, which can be cycled repeatedly. This feature consists of a highly reversible vesicle size change accompanied by diffusion of species into and out of vesicles. The "breathing" feature can be repeated many times, with relaxation time of ca. 1 min. The wall consists of three layers and is prepared from a triblock copolymer, poly(ethylene oxide)$_{45}$-*block*-polystyrene$_{130}$-*block*-poly(2-diethylaminoethyl methacrylate)$_{120}$ (PEO_{45}-b-PS_{130}-b-$PDEA_{120}$). The vesicle size, wall structure, thickness, and

(33) Ding, J. F.; Liu, G. J. *J. Phys. Chem. B* **1998**, *102*, 6107–6113.
(34) Lee, J. C. M.; Bermudez, H.; Discher, B. M.; Sheehan, M. A.; Won, Y. Y.; Bates, F. S.; Discher, D. E. *Biotechnol. Bioeng.* **2001**, *73*, 135–145.
(35) Photos, P. J.; Bacakova, L.; Discher, B.; Bates, F. S.; Discher, D. E. *J. Controlled Release* **2003**, *90*, 323–334.
(36) Lomas, H.; Canton, I.; MacNeil, S.; Du, J.; Armes, S. P.; Ryan, A. J.; Lewis, A. L.; Battaglia, G. *Adv. Mater.* **2007**, *19*, 4238–4243.
(37) Discher, D. E.; Ortiz, V.; Srinivas, G.; Klein, M. L.; Kim, Y.; David, C. A.; Cai, S. S.; Photos, P.; Ahmed, F. *Prog. Polym. Sci.* **2007**, *32*, 838–857.
(38) Pang, Z. Q.; Lu, W.; Gao, H. L.; Hu, K. L.; Chen, J.; Zhang, C. L.; Gao, X. L.; Jiang, X. G.; Zhu, C. Q. *J. Controlled Release* **2008**, *128*, 120–127.
(39) Chiu, D. T.; Wilson, C. F.; Karlsson, A.; Danielsson, A.; Lundqvist, A.; Stromberg, A.; Ryttsen, F.; Davidson, M.; Nordholm, S.; Orwar, O.; Zare, R. N. *Chem. Phys.* **1999**, *247*, 133–139.
(40) Nardin, C.; Thoeni, S.; Widmer, J.; Winterhalter, M.; Meier, W. *Chem. Commun.* **2000**, 1433–1434.
(41) Vriezema, D. M.; Garcia, P. M. L.; Oltra, N. S.; Hatzakis, N. S.; Kuiper, S. M.; Nolte, R. J. M.; Rowan, A. E.; van Hest, J. C. M. *Angew. Chem., Int. Ed.* **2007**, *46*, 7378–7382.
(42) Nallani, M.; de Hoog, H. P. M.; Cornelissen, J.; Palmans, A. R. A.; van Hest, J. C. M.; Nolte, R. J. M. *Biomacromolecules* **2007**, *8*, 3723–3728.
(43) Boerakker, M. J.; Botterhuis, N. E.; Bomans, P. H. H.; Frederik, P. M.; Meijer, E. M.; Nolte, R. J. M.; Sommerdijk, N. *Chem.—Eur. J.* **2006**, *12*, 6071–6080.
(44) Reynhout, I. C.; Cornelissen, J.; Nolte, R. J. M. *J. Am. Chem. Soc.* **2007**, *129*, 2327–2332.
(45) Wang, W.; McConaghy, A. M.; Tetley, L.; Uchegbu, I. F. *Langmuir* **2001**, *17*, 631–636.
(46) Adams, D. J.; Butler, M. F.; Weaver, A. C. *Langmuir* **2006**, *22*, 4534–4540.
(47) Jiang, Y.; Chen, T.; Ye, F. W.; Liang, H. J.; Shi, A. C. *Macromolecules* **2005**, *38*, 6710–6717.
(48) Azzam, T.; Eisenberg, A. *Angew. Chem., Int. Ed.* **2006**, *45*, 7443–7447.
(49) Harris, J. K.; Rose, G. D.; Bruening, M. L. *Langmuir* **2002**, *18*, 5337–5342.
(50) Sun, J.; Chen, X. S.; Deng, C.; Yu, H. J.; Xie, Z. G.; Jing, X. B. *Langmuir* **2007**, *23*, 8308–8315.
(51) Yu, Y. S.; Eisenberg, A. *J. Am. Chem. Soc.* **1997**, *119*, 8383–8384.
(52) Choucair, A.; Lavigueur, C.; Eisenberg, A. *Langmuir* **2004**, *20*, 3894–3900.
(53) Zhang, L. F.; Eisenberg, A. *Macromolecules* **1996**, *29*, 8805–8815.
(54) Zhang, X. J.; Wang, Y. L.; Wang, W. *Langmuir* **2009**, *25*, 2075–2080.
(55) Huang, J. B.; Zhu, Y.; Zhu, B. Y.; Li, R. K.; Fu, H. I. *J. Colloid Interface Sci.* **2001**, *236*, 201–207.
(56) Rangelov, S. *J. Phys. Chem. B* **2006**, *110*, 4256–4262.
(57) Li, X. F.; Kroeger, A.; Azzam, T.; Eisenberg, A. *Langmuir* **2008**, *24*, 2705–2711.
(58) Shen, H. W.; Eisenberg, A. *J. Phys. Chem. B* **1999**, *103*, 9473–9487.
(59) Luo, L. B.; Eisenberg, A. *Langmuir* **2001**, *17*, 6804–6811.
(60) Choucair, A. A.; Kycia, A. H.; Eisenberg, A. *Langmuir* **2003**, *19*, 1001–1008.
(61) Mai, Y. Y.; Zhou, Y. F.; Yan, D. Y. *Small* **2007**, *3*, 1170–1173.
(62) Du, J. Z.; Armes, S. P. *J. Am. Chem. Soc.* **2005**, *127*, 12800–12801.
(63) Checot, F.; Lecommandoux, S.; Gnanou, Y.; Klok, H. A. *Angew. Chem., Int. Ed.* **2002**, *41*, 1339–1343.
(64) Sigel, R.; Losik, M.; Schlaad, H. *Langmuir* **2007**, *23*, 7196–7199.
(65) Gebhardt, K. E.; Ahn, S.; Venkatatchalam, G.; Savin, D. A. *J. Colloid Interface Sci.* **2008**, *317*, 70–76.
(66) Shi, Z. Q.; Zhou, Y. F.; Yan, D. Y. *Macromol. Rapid Commun.* **2008**, *29*, 412–418.

appearance were studied in both the shrunken state (pH 10.4) and the expanded state (pH 3.4) by DLS, cryo-TEM, and regular TEM. Then the pH-related changes in vesicle size, wall thickness, structure, and appearance between the two extreme states were investigated; the mechanisms of these changes are discussed extensively. The kinetics of the size change and of the "breathing" feature was also studied. Finally, the permeability of the vesicle wall to water and protons was studied, and the changes in the proton diffusion coefficient at different pH values are explained on the basis of changes in the wall structure.

Experimental Section

For experimental details, please refer to the Supporting Information.

Results and Discussion

The Results and Discussion section of the paper is presented in seven parts. The first part, dealing with the synthesis of the triblock copolymer, is located entirely in the Supporting Information. In the subsequent parts of the section, the following topics are discussed: the process of the self-assembly of the copolymer into vesicles at pH 10.4; size, appearance, and morphology at pH 3.4; pH-sensitivity of vesicle size, wall thickness, wall structure, and appearance; mechanisms of the pH-induced changes; the "breathing" or cycling feature; and, finally, the transport of water and protons and the calculated permeability values.

1. Synthesis of Triblock Copolymer PEO_{45}-b-PS_{130}-b-$PDEA_{120}$. A discussion of the detailed synthesis route and characterization techniques is given in the Supporting Information.

2. Self-Assembly of PEO_{45}-b-PS_{130}-b-$PDEA_{120}$ into Vesicles: Size and Morphology at pH 10.4. Before discussing the self-assembly of the triblock copolymer, it is useful to recall that the pK_a of the poly(2-diethylaminoethyl methacrylate) is approximately 7.5,[67] and the polymer is insoluble in water when the pH exceeds the neutral range.[68] It is also worth recalling that the hydrophobic to hydrophilic block length ratio should be relatively high to obtain vesicles.[1] The relative number of hydrophobic to hydrophilic units, i.e., 250 hydrophobic (PS_{130} + $PDEA_{120}$ when pH > 8.6) to 45 hydrophilic, coupled with the large size of the hydrophobic styrene units relative to that of ethylene oxide, suggests that PEO_{45}-b-PS_{130}-b-$PDEA_{120}$ might be in the vesicle range. This was confirmed in preliminary experiments. Specifically, it had been determined earlier that PEO_{45}-b-PS_{235} was a vesicle former, and the triblock was similar to that material in terms of the relative hydrophobic to hydrophilic block lengths. The self-assembly was performed under strongly basic conditions (pH higher than 10.4) to ensure that the PDEA remains insoluble and, thus, that it behaves like a hydrophobic unit along with polystyrene. It had been shown previously that acids or bases can change morphologies in PS-b-PAA diblock.[69] It should be noted that since, under preparation conditions, the present system is not near a morphological boundary, the presence of base does not alter the morphology.

The aggregates prepared at pH 10.4 were first analyzed by dynamic light scattering. The results of this study, along with those of the EM investigation, are given in Figure 1. The angular dependence of the diffusion coefficient D_{diff} plotted against the square of the scattering vector q, as determined by DLS, is shown in Figure 1a. A slight angular dependence is seen in the plot; the hydrodynamic radius R_h, calculated from the extrapolation of D_{diff} to 0° angle, is found to be 240 nm. R_h was also measured at an angle of 90° and analyzed by the CONTIN mode to be approximately 250 nm, i.e., very close to the R_h at $q = 0$. In view of this agreement, all the remaining experiments were performed at an angle of 90° unless special conditions were encountered. The size distribution determined from the measurement at an angle of 90° is shown in Figure 1b.

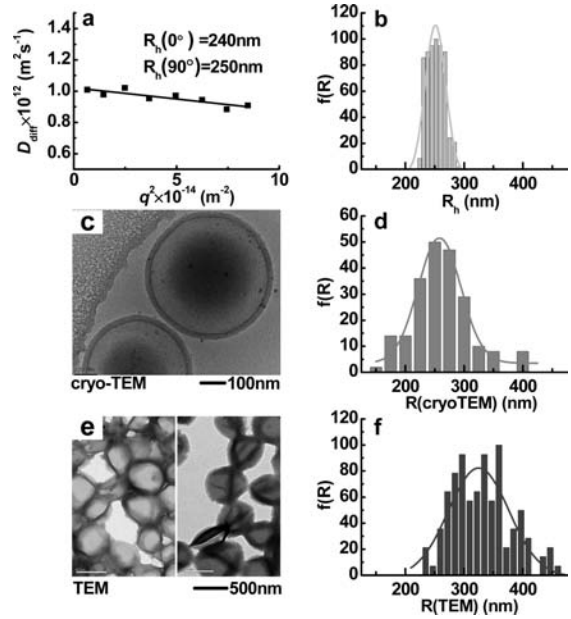

Figure 1. Analysis of vesicles prepared at pH 10.4 from DLS and EM studies. (a) Angular dependence of the diffusion coefficient (D_{diff}) on scattering vector (q^2); (b) hydrodynamic radius (R_h) distribution (scattering angle = 90°) of the vesicle solution; (c) cryo-TEM image of vesicles; (d) statistical size distribution counted from 18 vesicles in the cryo-TEM images; for each vesicle, multiple measurements were made in different directions; (e) TEM images of vesicles prepared from solution and dried in air (left) and under vacuum (right); (f) statistical size distribution counted from more than 50 vesicles in the TEM image. Gray solid lines in b, d, and f are Gauss fitting curves of the presented data. The scale of the horizontal axes in b, d, and f is the same.

The aggregates were also investigated by electron microscopy. Figure 1c shows a typical cryo-TEM image of the aggregates prepared at pH 10.4 and clearly indicates that the aggregates are vesicles with an intact wall. Figure 1d shows the statistical radius distribution of the vesicles counted from 18 vesicles with each vesicle measured at multiple angles in the cryo-TEM images; the z-average radius, calculated from the distribution, is approximately 260 nm, which is in good accord with that obtained by DLS (R_h = 240 nm at q = 0). In view of the agreement, these images were also used to measure the wall thickness δ_w, and the statistical result on the 18 vesicles yields a thickness of ca. 25 nm at pH 10.4 (see Figure S5 in the Supporting Information). At the same time, the wall thickness, δ_w, of the vesicles prepared from the precursor diblock copolymer PEO_{45}-b-PS_{130} under identical conditions was also measured from seven vesicles in cryo-TEM images to yield a value of 13 nm. The comparison of the two wall thicknesses, 25 nm from the vesicles formed by the triblock and 13 nm from that formed by the diblock, implies that both PS and PDEA blocks participate in the formation of the vesicle wall under

(67) van de Wetering, P.; Moret, E. E.; Schuurmans-Nieuwenbroek, N. M. E.; van Steenbergen, M. J.; Hennink, W. E. *Bioconjugate Chem.* **1999**, *10*, 589–597.
(68) Butun, V.; Armes, S. P.; Billingham, N. C. *Polymer* **2001**, *42*, 5993–6008.
(69) Zhang, L. F.; Yu, K.; Eisenberg, A. *Science* **1996**, *272*, 1777–1779.

the experimental conditions. Further details on the wall structure will be given in the following sections.

Figure 1e shows regular TEM images of the vesicles prepared at the same pH but dried on the EM copper grids either in air or under vacuum, respectively. Again, vesicles are observed, which, however, apparently collapsed, possibly when air was admitted after evacuation. The size distribution from the TEM images of the air-dried vesicles is shown in Figure 1f on the same scale as that of Figure 1d and 1b to allow a direct comparison of the sizes; the *z*-average radius calculated from the distribution is approximately 340 nm. It is clear that the size obtained from TEM ($\approx$ 340 nm) is considerably larger than that obtained from cryo-TEM ($\approx$ 260 nm), which is very close to that obtained from DLS at $q = 0$ ($\approx$ 240 nm) and at an angle of 90° ($\approx$ 250 nm). The increase in size in Figure 1f is probably due to the flattening of vesicles on the EM grid during drying. A calculation, given in the Supporting Information, shows that the increase in size resulting from the collapse of a hollow sphere to a pancake should be 41% and indicates that the vesicles collapsed into pancakes in the process of drying. The average radius from cryo-TEM (340 nm) compared with that from air-dried vesicles in Figure 1e (260 nm) suggests an increase in size of ca. 30%. In view of the fact that the vesicles in Figure 1e are not separated from each other and also that some of them are "wrinkled" and therefore cannot collapse completely to a pancake, the agreement (~30% vs 41%) can be considered satisfactory. The images in Figure 1e were not considered precise enough for measurements of wall thickness.

The analysis results from Figure 1 clearly show that the aggregates prepared from the triblock copolymer PEO_{45}-b-PS_{130}-b-$PDEA_{120}$ at pH 10.4 are vesicles with a homogeneous appearance and an intact wall. The DLS analysis also gives a radius of approximately 250 nm, while cryo-TEM gives a thickness δ_w of ca. 25 nm in solution; it is also seen that the vesicles collapse to pancakes with an average radius of about 340 nm when dried.

3. Vesicle Size, Appearance, and Wall Structure at pH 3.4. The presence of the PDEA segment in the wall suggests that the vesicles should be pH-sensitive; this was, indeed, found to be the case, and the results will be discussed in the subsequent section. In the present section, the vesicle size, appearance, and wall structure at pH 3.4 are described. At that pH, the vesicles are at their maximum size and, thus, represent the other extreme of the "breathing" mode. As before, the vesicles were studied by DLS and EM, and the results are shown in Figure 2. The diffusion coefficient D_{diff}, as a function of q^2, is plotted in Figure 2a. The R_h calculated from the extrapolation of D_{diff} to 0° angle yields a value of 480 nm, while R_h analyzed by the CONTIN mode at 90° yields a value of 460 nm. The DLS results suggest that the vesicles also show a slight angular dependence of R_h here. The size distribution of R_h at this pH is presented in Figure 2b.

A typical cryo-TEM image of the vesicles at pH 3.4 is given in Figure 2c. Compared with its counterpart at pH 10.4 (Figure 1c), the vesicle size has increased dramatically; the structure of the vesicle wall has also become much more complicated. First, the wall now consists of two somewhat irregular dark lines and one continuous gray region between them. Recalling the electron density difference between the wall-forming blocks, PS and PDEA, it seems reasonable to identify the dark lines as the PS layers and the gray region as the PDEA layer. The contrast between the dark lines and the gray region suggests there is a relatively sharp boundary between the PS layers and the PDEA

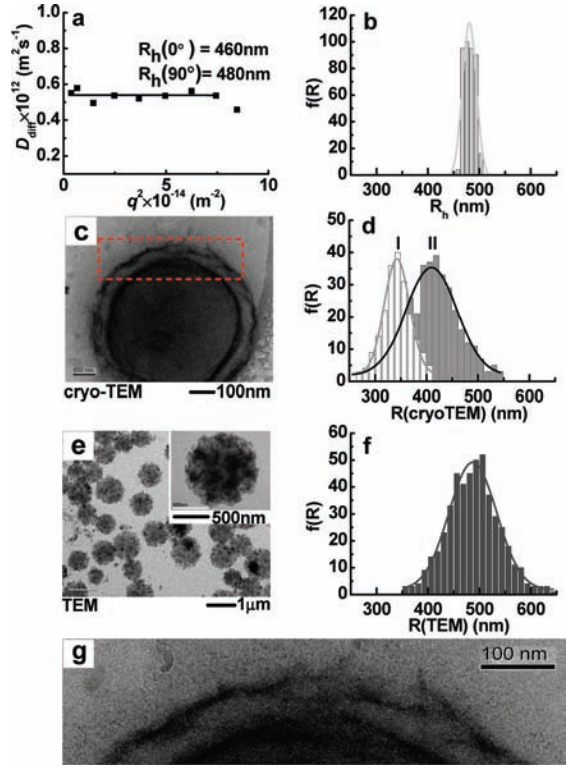

Figure 2. Analysis of vesicles at pH 3.4 by DLS and EM studies. (a) Angular dependence of diffusion coefficient (D_{diff}) on scattering vector (q^2); (b) hydrodynamic radius (R_h) distribution (scattering angle = 90°) of the vesicle solutions; (c) cryo-TEM image of vesicles; (d) statistical size distribution counted from 15 vesicles in the cryo-TEM images with multiple measurements for each vesicle in different directions (I, from the vesicle center to the edge of the external PS layer; II, from the vesicle center to the end of extruded PDEA chains); (e) TEM image of vesicles prepared from solution and freeze-dried under vacuum; (f) statistical size distribution counted from more than 50 vesicles in the TEM image; (g) enlarged cryo-TEM image of the area enclosed by dash lines in c. Gray solid lines in b, d, and f are Gauss fitting curves of the presented data. The scale of the horizontal axes in b, d, and f is identical to allow comparison.

layer, presumably due to the immiscibility between the hydrophobic PS block and the now hydrophilic and water swollen PDEA block. Second, some irregularities are also seen outside but close to the external dark line (see enlarged image in Figure 2g), which represents the external PS wall. It should be noted that the two PS layers are discontinuous; the darker irregularities are identified as PDEA chains extruded from the intermediate PDEA layer through the discontinuities or "cracks" in the PS layers. Summarizing the above analysis, it is now possible to describe the structure of the vesicle wall at pH 3.4 as consisting of three layers: two thin cracked PS layers on the wall surfaces and one PDEA layer in the middle, with some chains extruded through the cracks in the PS layers into the solution. It is worth noting that the "sandwich-like" three-layered wall structure (plus corona layers on each side) at pH 3.4 is not similar either to the one-layer wall structure with corona chains on each side, which is often seen in diblock copolymer vesicles,[1,48] or to the two-layer wall structure formed by a ABCA tetrablock copolymer with two immiscible hydrophobic blocks B and C.[70]

Cryo-TEM images at pH 3.4 have been analyzed in the following two ways: one way is to measure the radial distance from the center of the vesicle to the edge of the external PS

(70) Brannan, A. K.; Bates, F. S. *Macromolecules* **2004**, *37*, 8816–8819.

layer; the other way is to measure that from the center to the end of the extruded PDEA chains. The statistical size distribution obtained from the first way is shown as curve I in Figure 2d (white columns), for which the average radius is 340 nm. The distribution obtained from the second method is shown as curve II in Figure 2d (dark gray columns), with the average radius of 410 nm. The first radius value (340 nm) is much lower than that obtained from DLS, while the second value (410 nm) is comparable. The difference between the two radii, 340 vs 410 nm, may be attributed to the extrusion of the PDEA chains. The wall thickness δ_w is measured to be *ca.* 80 nm from the cryo-TEM images (see Figure S5 in the Supporting Information), which is clearly much greater than that at pH 10.4 ($\approx$ 25 nm). The obvious swelling of the intermediate PDEA layer is responsible for the dramatic size increase.

The surface discontinuities are also reflected in the TEM images. Figure 2e shows a typical TEM image of the vesicles freeze-dried at pH 3.4 with an enlarged vesicle in the inset. The TEM images here show a very mottled appearance, suggesting heterogeneities across the surface, which is quite unlike the partly folded structures resulting from the irregular collapse of the vesicles at pH 10.4 (Figure 1e). Keeping in mind the image in Figure 2c, the mottled appearance here is probably caused by the overlapping of the fragments of the PS layers, when vesicles are flattened onto the copper grids during drying. The dark regions in Figure 2e probably reflect the overlap of several PS layers (as many as four are possible), while the lighter regions may reflect less PS and more open space, i.e., the cracks.

Figure 2f shows the statistical size distribution, which is obtained by counting more than 50 vesicles at multiple angles in the TEM images. The *z*-average radius is found to be 490 nm from the distribution. This time, the radius seems very close to the R_h measured by DLS. This value also happens to be ca. 40% greater than the average radius of 340 nm, measured in the cryo-TEM images from the center of the vesicle to the edge of the external PS layer. Recalling the size increase percentage (41%), when a sphere collapses to a pancake during drying (see Scheme S2 in the Supporting Information), it is reasonable to suggest that the radius measured from TEM images is the one for the pancakes, into which the vesicles collapse at pH 3.4 when dried. TEM observations were also made at several angles; the circles change into ellipses with increasing angle, which confirms the flattened structure.

4. pH-Induced Changes of Vesicle Size, Wall Thickness, Appearance, and Structure. The results shown in Figures 1 and 2 reveal significant differences in size, wall thickness, appearance, and even the wall structure of the vesicles at pH 10.4 and 3.4. These differences originate from the differences in the nature of the pH-sensitive PDEA block at different pH values. In the present section, these pH-induced changes will be described for the pH range from 10.4 down to 3.4, the two extreme pH values that mark the beginning and end of the "breathing" mode. Experimentally, the study was started at pH 10.4, and then the pH was decreased by the stepwise addition of HCl. After each HCl addition, two hours were allowed for equilibration. At each step, the size was monitored by DLS. At six pH values, the appearance was also monitored by cryo-TEM, the wall thickness was measured from the cryo-TEM images, and the wall structure was analyzed.

First, the measured R_h of the vesicles (from DLS) and the wall thickness δ_w (from cryo-TEM) are plotted against solution pH in Figure 3. The two curves show strikingly similar shapes; both consist of two segments with obvious discontinuities at a pH of ca. 6: one segment extends from pH 10.4 down to 6, while the other covers the range from pH 6 down to 3.4. In the first part, R_h increases by approximately 35% (from 250 nm to 340 nm) and the wall thickness δ_w increases by ca. 60% (from 25 nm to 40 nm). In the second part, the R_h increases further for a total increase of ca. 90% (from 250 nm to 480 nm) and δ_w increases by 40 nm to a total percentage of ca. 325% (from 25 nm to 80 nm). The shape of the R_h curve from pH 10.4 down to pH 6 resembles that seen for vesicles with pH-sensitive PDEA segments restricted in a cross-linked wall network, and the size increase percentage is also close to the reported value.[62] Wall thicknesses were not reported in the literature; thus comparisons are impossible.

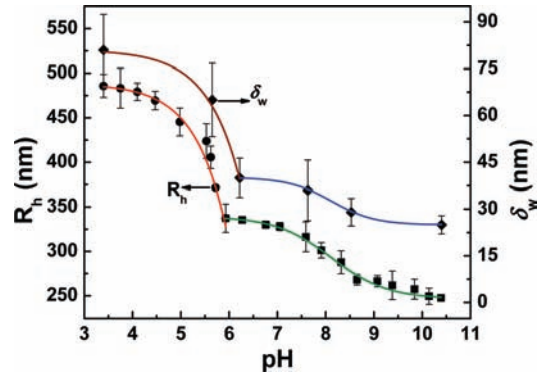

Figure 3. Dependence of R_h and wall thickness δ_w on the solution pH. δ_w was measured from cryo-TEM images with wall thickness in each vesicle measured many times in different places. Fittings are made by a sigmoidal model ($y = (A_1 - A_2)/[1 + e^{(x - x_0)/dx}] + A_2$) from pH 10.4 to 6 or exponential decay model ($y = y_0 + Ae^{-x/b}$) from pH 6 to 3.4, and the fitting results are shown in solid lines.

In addition to the size and wall thickness, the appearance and wall structure of the vesicles were also investigated at pH 10.40, 8.53, 7.63, 6.22, 5.65, and 3.40. Wedge-shaped sections of the cryo-TEM images at these pH values are shown in Figure 4, along with the schematic illustrations of the observed images and the thickness values of each layer (in the table). It is seen that the vesicle wall has a different appearance at these pH values: intact walls were observed at pH 10.40, 8.53, 7.63, and 6.22, while apparent discontinuities were found at pH 5.65 and 3.40.

With regard to the wall structure, all of the cryo-TEM images in Figure 4a show a similar "dark−gray−dark" three-layered structure in the entire pH range from 10.40 down to 3.40. The dark lines are interpreted as the PS layers, and the intermediate gray region is interpreted as the PDEA layer. Such a visible three-layered wall structure presented here is in agreement with the theoretical simulation results for a weakly segregated linear triblock copolymer system.[71] Apparent differences for different pH values are seen in Figure 4a regarding the thickness of the PS layer δ_{PS}, the continuity of the PS layers, and the thickness of the PDEA layer δ_{PDEA}. Figure 4a shows that, as the pH changes from 10.4 down to 3.40, the two PS layers change from very thin continuous layers at pH 10.40 and 8.53, to "bumpy" but still continuous layers at pH 7.63, then to uniform thicker continuous layers at pH 6.22, and finally to thick and broken layers at pH 5.65 and 3.40. As to the PDEA layer, it is found that it remains continuous over the entire pH range, while increasing in thickness. Some PDEA chains may have been

(71) Wang, R.; Tang, P.; Qiu, F.; Yang, Y. L. *J. Phys. Chem. B* **2005**, *109*, 17120–17127.

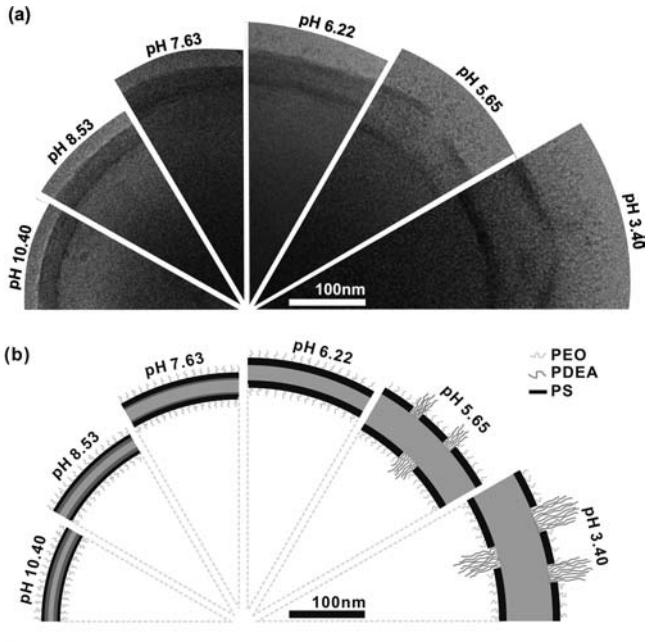

(c)

Thickness (nm)	pH 10.40	pH 8.53	pH 7.63	pH 6.22	pH 5.65	pH 3.40
δ_{PS}	4	5	7	10	10	10
δ_{PDEA}	17	19	21	20	45	61
δ_{w}	25	29	36	40	65	81

Figure 4. (a) cryo-TEM images of vesicle wall structures at pH 10.4, 8.53, 7.63, 6.22, 5.65, and 3.40, respectively; (b) schematic illustrations of the vesicle structures at corresponding pH values; (c) thickness values of the PS layer δ_{PS}, the PDEA layer δ_{PDEA}, and the wall δ_{w}. δ_{w} and δ_{PS} were measured from the cryo-TEM images directly (see Figure S6 in the Supporting Information for measurement illustrations), while δ_{PDEA} is calculated by the equation $\delta_{PDEA} = \delta_{w} - 2 \times \delta_{PS}$.

extruded through the cracks in the PS layers into the solution at pH 6.22, and more chain extrusions via the "cracks" in the PS layers are seen at pH 5.65 and 3.40.

5. Mechanisms of Changes in Wall Structure, Appearance, Thickness, and Vesicle Size. As described above, varying the solution pH induces significant changes in vesicle sizes, wall thickness (Figure 3), and the wall structure and appearance (Figure 4a). These changes over the entire pH region (10.4−3.4) originate from the protonation of the amino groups in the PDEA chains and the accompanying hydration, i.e., swelling of the PDEA chains. It is also apparent that these changes can be divided into two regions by a threshold pH value of approximately 6. In the first region (pH 10.4−6), the PDEA layer swells between the two PS layers; in the second region (pH 6−3.4), the PDEA layer swells within a much less restricted environment, because the PS layers crack at pH below 6 in response to the increasing swelling pressure. In the following section, we focus on how the swelling of the PDEA layer in the two pH regions influences the wall structure, appearance, thickness, and vesicle size.

The vesicle wall structure is discussed first. The cryo-TEM images in Figure 4a show that the vesicle wall consists of two PS layers and one intermediate PDEA layer. The layer structure is, undoubtedly, a result of the immiscibility between the two materials; thus, any factor that can change their miscibility may induce the change in the wall structure. At the initial pH (10.4), the immiscibility between the two hydrophobic blocks, the PS and the PDEA, leads to the formation of the three-layered structure. The PS layer is found to be ca. 4 nm thick, while the middle PDEA layer is calculated to be 17 nm thick. The two values agree well with the results calculated from stoichiometric consideration, i.e., the aggregation number, block length, and densities of PS and PDEA, with $\delta_{PS} \approx 5$ nm and $\delta_{PDEA} \approx 15$ nm (see Supporting Information). Thus, the measured results are considered reasonable. When the solution pH decreases from 10.4, the PS chains remain hydrophobic, while the PDEA chains become progressively protonated and hydrophilic and consequently hydrated. Thus, with decreasing pH, there is an increasingly stronger tendency for phase separation between the two materials. The table in Figure 4c shows progressively increasing thickness of both the PS layers and the PDEA layer. It is understandable that the increase of δ_{PDEA} is the direct result of the swelling of the PDEA chains; by contrast, it is not easy to understand the increase of δ_{PS}.

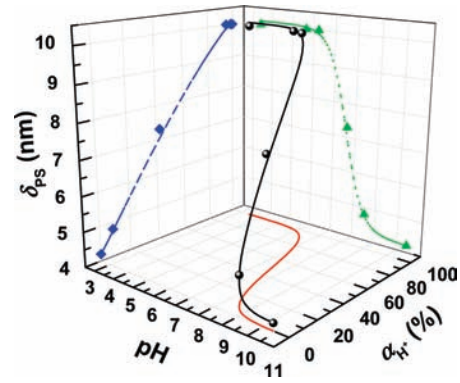

Figure 5. Relationship between the PS layer thickness δ_{PS}, the degrees of protonation α_{H^+}, and the solution pH. δ_{PS} was measured from the cryo-TEM images (see Figure S6 in the Supporting Information for measurement illustrations). α_{H^+} was calculated by the equation $\alpha_{H^+} = 1/(1 + 10^{pH-pKa})$, and pK_a is assumed to be 7.5, the same as that of the PDEA homopolymer.[67,68] The points in these plots are experimental, while the curves are fitted by a sigmoidal model or exponential decay model (see Figure 3 for equations) except the α_{H^+} curve.

A 3-D plot of δ_{PS} versus the degree of protonation α_{H^+} of the amino groups in PDEA chains versus the solution pH is shown in Figure 5. It has to be pointed out that α_{H^+} used here is only an approximation because it was calculated from data for PDEA homopolymer.[67,68] Figure 5 shows almost identical changes of δ_{PS} and α_{H^+} versus pH: both increase slowly in the pH range from 10.4 to 9, then steeply from pH 8.5 to 6.5, and finally to a plateau at pH 6 and below. The two curves show very close inflection points. These similarities strongly suggest that the increase of δ_{PS} is closely related to the protonation and hydration of the PDEA layer, which occurs at low pH. It is tempting to suggest that the apparent increase in the thickness of the PS layers with decreasing pH is related to the increasing incompatibility between the PS and the hydrated PDEA. At high pH, the PDEA and PS are both hydrophobic; therefore, it seems reasonable to suggest that the interfacial region would be relatively broad. However, as the pH decreases, the PDEA layer becomes protonated and hydrated, the incompatibility increases, and the interfacial layer becomes much sharper. This probably results in the increase of the apparent thickness of the two PS layers.

A brief explanation is given here to rationalize the pH-induced changes in the structures of the vesicle walls. The PS−PDEA−PS three-layered wall structure is initially formed during vesicle preparation in a mixed solvent at high pH due to the hydrophobicity of both the PS and PDEA and the apparent immiscibility between them. As the pH decreases, the intermediate

PDEA layer becomes protonated and hydrated; swelling of this layer is therefore to be expected, and the thickness increase of this layer is, indeed, seen in the cryo-TEM images. The swelling of the PDEA layer further increases the immiscibility between the PDEA and PS (because of an increase in the hydrophilic nature of the hydrated PDEA) and thus sharpens the interface between them; consequently, an apparent increase of thickness of PS layers is seen in the cryo-TEM images. When the pH decreases to 6, the vesicle size increases by 35% (from 250 nm at pH 10.4 to 340 nm at pH 6), and on further pH change to 3.4 by a total of ca. 90% (from 250 nm at pH 10.4 to 470 nm at pH 3.4); the average surface area of the vesicles increases by ~80% ($1.35 \times 1.35 \approx 1.80$) by pH 6 and finally by 260% ($1.90 \times 1.90 \approx 3.60$) by pH 3.4. The PS layers cannot sustain such an expansion and, therefore, crack to release the swelling pressure from the intermediate PDEA layer. Throughout the swelling/deswelling processes, the PDEA layer remains intact, with the PS sections fragmenting and reconnecting on swelling and deswelling.

Following the above analysis, a detailed description of the vesicle structure becomes possible. At the initial pH 10.4, as one moves from the outside solution to the center of vesicles, one would meet a PEO corona layer, a thin continuous PS layer, a relatively wide PS−PDEA interface layer, a PDEA layer, a second relatively wide PDEA−PS interface layer, a second thin PS layer, and finally a second PEO corona layer. As the pH decreases, the thin PEO corona layers remain, but between those layers, one would encouter a thickening PS layer, a narrowing PS−PDEA interface layer, a thickening PDEA layer due to the swelling, a second narrowing PDEA−PS interface layer, and a second thickening PS layer. When the pH drops to 6 and below, one would probably find a 10 nm intact (pH > 6) or broken (pH < 6) PS layer, a very thick continuous PDEA layer, and a second 10 nm intact or fragmented PS layer. The detailed structures of the vesicles described above are illustrated in Figure 4b.

The change in the appearance of the vesicle wall will now be described, since the change is closely related to that of the three-layered wall structure. At the initial pH of 10.40, the PDEA chains are neither hydrated nor protonated; the PDEA layer is in a nonswollen state. Although the PDEA layer is retained within the two PS layers, no stress is applied to the PS layers. The vesicle walls show a smooth profile of the surface (Figure 4, pH = 10.40). When HCl is added to the solution to lower the pH, the PDEA chains start to be protonated and hydrated, so the layer swells. It has to be pointed out that the PS layers are only several nanometers thick (Figure 5). In this case, the T_g of the thin PS layers is probably lower than that of bulk PS materials (see Figure S7 in Supporting Information),[72−74] so the PS layers are not in a glassy state, but in a rubbery state. Therefore, the two PS layers can be passively expanded due to the stress from the intermediate swollen PDEA layer. Within this pH range, walls with intact surfaces are seen (Figure 4, pH 8.53, 7.63, 6.22). It is also suggested that the T_g of the two thin PS layers increases rapidly with increasing δ_{PS} and finally reaches ~50 °C, where $\delta_{PS} = 10$ nm (pH = 6.22 and below). At that point, the PS chains are in the glassy state, and the PS layers have lost their possibly rubber-like elasticity. In this case, any further increase of stress from the swollen PDEA layer could rupture the two PS layers. Therefore, at pH values below 6, a wall with a fragmented surface is seen along with polymer chains extruded into the solution through the "cracks" in the PS walls (Figure 4a, pH 5.65 and 3.40).

Figures 3 and 4 show that the wall thickness δ_w, the thickness of the PS layer δ_{PS}, and that of the PDEA layer δ_{PDEA} are all pH-sensitive. This pH-dependence of the thickness will be discussed here. The total δ_w is known to consist of the thickness of the two PS layers ($2 \times \delta_{PS}$) and the thickness of the PDEA layer (δ_{PDEA}), i.e., $\delta_w = 2 \times \delta_{PS} + \delta_{PDEA}$. Over the entire pH range (10.4−3.4), δ_w increases totally by 56 nm (from 25 nm to 81 nm), δ_{PDEA} increases by 44 nm (from 17 nm to 61 nm), and δ_{PS} increases by 6 nm (from 4 nm to 10 nm) (see the table in Figure 4c). As was suggested before, the increase of δ_{PDEA} arises from the swelling of the PDEA layer with decreasing pH due to protonation and hydration; the increase of δ_{PS} is most likely the result of the increasing incompatibility between the hydrophobic PS and the swollen PDEA. The increase of δ_{PDEA}, 44 nm, is found to represent 79% of the increase of δ_w, while the total increase of the thickness of the two PS layers, 12 nm, is found to represent only 21% of the increase of δ_w. As might be expected, the swelling of the intermediate PDEA layer has a decisive influence on the increase of the wall thickness over the whole pH range (10.4−3.4).

Further analysis on the change of δ_w in Figure 3 reveals that the swelling of the PDEA layer shows different influences in different pH regions. In the first, or high, pH region (pH 10.4−6), δ_w increases by 15 nm (from 25 nm to 40 nm), δ_{PS} increases by 6 nm (from 4 nm to 10 nm), and δ_{PDEA} increases 3 nm (from 17 nm to 20 nm). The sum of the increases from the two PS layers, 12 nm, contributes 77% to the increase of the wall thickness, while the increase from the PDEA layer, 3 nm, contributes only 33%. Therefore, the increase of δ_w in this pH range is controlled by the increase of δ_{PS} of the two PS layers; the swelling of the intermediate PDEA layer is surprisingly low and appears to be constrained by the two PS layers. In the second or low pH region (pH 6−3.4), δ_{PS} shows essentially no increase (~10 nm); so δ_w and δ_{PDEA} both show an almost identical burst increase when pH decreases to just below 6. δ_w then reaches a plateau as the pH approaches 3.4; the increase is 41 nm (from 40 nm to 81 nm). The burst increase of δ_{PDEA} probably arises from the sudden rupture of the PS layers due to the loss of rubber-like elasticity, and the further increase of δ_{PDEA} is the result of the further protonation and hydration. Therefore, from pH 6 to 3.4, the increase of δ_w is totally dominated by the swelling of the PDEA layer. Summarizing these details, it follows that, in the pH range of 10.4 to 6, the increase of the vesicle wall thickness is constrained by the two PS layers, while in the low pH range of 6 to 3.4, the increase is totally controlled by the swelling of the PDEA layer.

The next part deals with the change of the vesicle size and the persistence of the vesicle shape. The similarity of the two curves in Figure 3 raises the question whether the swelling is homogeneous, i.e., whether the change of the whole vesicle size is the same as the change of the wall thickness. To explore this aspect, two graphs were made by plotting $R_h/R_{h,pH=10.4}$ versus $\delta_w/\delta_{w,pH=10.4}$ for pH > 6, and $R_h/R_{h,pH=6}$ versus $\delta_w/\delta_{w,pH=6}$ for pH < 6, shown as $R_h/R_{h,ref}$ versus $\delta_w/\delta_{w,ref}$ in Figure 6. If the swelling were completely homogeneous, the slope should be 1. However, for the high pH range, the slope is 0.55, while for the low pH range it is 0.43. This shows that the swelling is not homogeneous. Clearly, the wall swells more strongly than the

(72) Keddie, J. L.; Jones, R. A. L.; Cory, R. A. *Europhys. Lett.* **1994**, *27*, 59–64.
(73) Erichsen, J.; Dolgner, K.; Zaporojtchenko, V.; Faupel, F. *Macromolecules* **2004**, *37*, 8813–8815.
(74) Chow, T. S. *J. Phys.: Condens. Matter* **2002**, *14*, l333−l339.

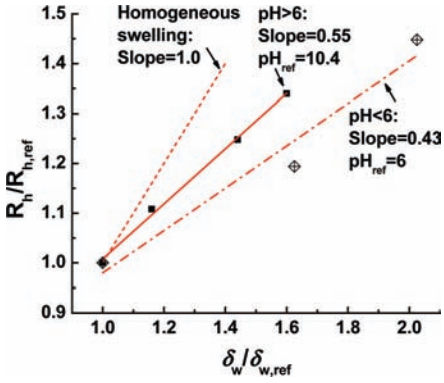

Figure 6. Relationship between the relative vesicle size increase ($R_h/R_{h,ref}$) and the relative vesicle wall thickness increase ($\delta_w/\delta_{w,ref}$). For pH < 6, the reference point is pH 6, while for pH > 6, the reference point is pH 10.4. A calculated line of a homogeneously swollen vesicle is also shown (dashed line) for comparison (see Supporting Information for the calculation details). The slope of each line is also indicated.

whole vesicle. The difference is not surprising, since the swelling of the whole vesicle is probably impeded by the PS layers. By contrast, no such impediment is encountered within the wall, so radial swelling of the wall is less constrained than the lateral swelling of the vesicle as a whole.

Regarding the size change itself, one may question why the vesicle size increases with increasing hydrophilic weight fraction (the progressively protonated PDEA chains), instead of the expected opposite trend reported by Jain and Bates.[75] The crucial point here is that the vesicles in the present study remain intact (although with cracks in the PS) throughout the pH changes. If the vesicles were to fall apart and re-form, or if they were to be assembled from single chains under equilibrium conditions in solutions of different pH, then the size relationship, as reported by Jain and Bates, would most likely be valid. However, once the vesicles are made at high pH, they obviously stay intact throughout the pH-induced size changes. Thus, the only freedom available to them is to swell or deswell, not to disassemble and reorganize to different vesicles, via a single chain intermediate mechanism.

Finally, it is also reasonable to question why the vesicle, once formed at high pH, does not reorganize to form a vesicle with a single layer wall and an asymmetric corona after a pH decrease. After all, Stoenescou and Meier[76] studied the biamphiphilic block copolymer poly(ethylene oxide)-*block*-poly(dimethylsiloxane)-*block*-poly(2-methyloxazoline) (written as PEO-b-PDMS-b-PMOXA), which yields a vesicle with a single-layer PDMS wall and an asymmetric corona, with PEO on the one side and PMOXA on the other side. In principle, at low pH, PDEA also becomes hydrophilic, so one could argue that we have an analogous system, and we should expect analogous behavior. To understand the difference in behavior, it should be born in mind that the difference in T_g between PS and PDMS is 220 °C. Bulk PDMS at room temperature is ca. 140 °C above its T_g, while bulk PS is ca. 75 °C below it. For this reason, and possibly also because of the difference in the hydrophilic and hydrophobic nature of the block copolymers involved, the vesicles with a PDMS wall can reorganize at room temperature in water, while those with PS cannot. After all, it is known that the polymers studied by Stoenescou and Meier form vesicles in pure water at room temperature. By contrast, PS-b-PEO or PS-b-PAA diblocks yield vesicles at room temperature only after the dissolution in a common solvent and the addition of water. Thus, since sizable chunks of the cracked PS wall remain intact upon swelling of the present system, the vesicle remains whole and cannot reorganize to form a single PS-walled vesicle.

6. The "Breathing" Feature. The kinetics of the pH-induced vesicle size change was studied in the same pH range as that used in the other studies, i.e., from 10.4 to 3.4. Experimentally, the real-time vesicle size was monitored by DLS upon the addition of HCl. The results are shown in Figure 7a. It is found that the vesicle size increases rapidly upon the addition of HCl and then reaches a plateau. When the curve is fitted with an exponential decay function (similar to that used to fit the data in Figure 3; the function is $y = y_0 + Ae^{-t/\tau}$), it yields a relaxation time τ of ~1.6 min. It should be pointed out that the attempt to determine the relaxation time by DLS is associated with considerable error; however, the value obtained is still instructive. Since changes of the wall structure, thickness, and appearance are probably all synchronous, τ should be the relaxation time for all these changes also.

Perhaps the most remarkable feature of the vesicles described here is the high degree of reversibility of pH-induced size changes. Experimentally, once the size reaches equilibrium after the addition of HCl at pH 3.4, the pH can be changed back to 10.4 by rapid addition of NaOH, and the size change can also be monitored by DLS. The size decrease is plotted in Figure 7a. The relaxation time τ was determined to be ca. 0.7 min. The pH cycling can be repeated many times, as shown on the bottom of Figure 7 for nine cycles. In each of the steps, the amount of HCl or NaOH added was exactly the same. It should be remembered that the total volume of the solution is 5 mL, while each addition of HCl or NaOH is only 8 μL. Thus, the total volume of solution changes only negligibly and the same amount of HCl or NaOH will yield the same final pH. It should also be pointed out that if one wishes to interrupt the cycling, it is important to do so with the vesicles at high pH, i.e., with the polystyrene shells in the "healed" condition rather than at low pH while the polystyrene shells are cracked. It has been observed that if one stores the vesicle solution for a long time at low pH, some degeneration occurs, so a high degree of reversibility will not be attained; by contrast, if one stores the vesicle solution at high pH, the size changes are highly reversible. In addition to monitoring the size change by DLS, the appearance of the vesicles was also investigated by TEM during pH cycling. Typical TEM images in both low pH and high pH states of the first and fourth cycle, as well as the last cycle, are shown in Figure S8 in the Supporting Information to illustrate the fact that the changes are highly reversible. Because of the repeatability of the size changes and associated transport phenomena, the term "breathing" seems appropriate.

It should be recalled that the vesicle size changes approximately by a factor of 1.9 upon the addition of HCl or NaOH within ca. 2 min, which means that a relatively large amount of water diffuses rapidly into or out of the vesicle interior during pH cycling. It should be recalled that the vesicle size change is also accompanied by changes of the wall thickness and structure; thus a precise calculation of the diffusion coefficient D would be extremely difficult. Here, we only calculate the initial diffusion coefficients, i.e., the point at which vesicles start to increase their size upon the addition of HCl or to decrease their size upon addition of NaOH. The calculation is based on the initial slope of volume change of the vesicle interior with time, the average surface area of the vesicles at

(75) Jain, S.; Bates, F. S. *Science* **2003**, *300*, 460–464.
(76) Stoenescu, R.; Meier, W. *Chem. Commun.* **2002**, 3016–3017.

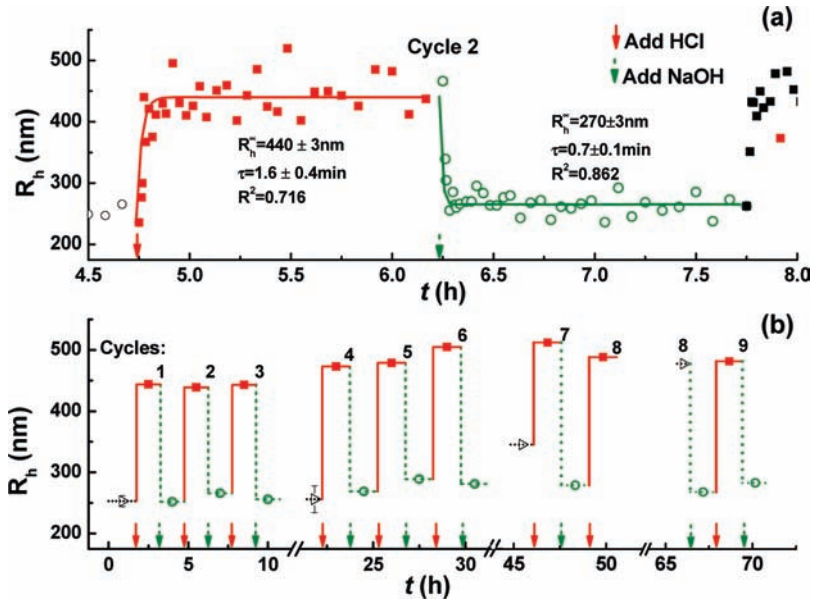

Figure 7. Time course of vesicle size change from DLS upon the addition of HCl or NaOH in the second cycle (a) and the cycle changes of vesicle size in response to the quick addition of HCl or NaOH (b). Arrows indicate points of addition of HCl or NaOH.

the starting point, pH 10.4 or 3.4, and the wall thickness at these pH values (see Supporting Information for details). The results reveal that the initial diffusion coefficients are ca. 3×10^{-13} and 3×10^{-12} $cm^2 \cdot s^{-1}$ upon addition of HCl and NaOH, respectively. The latter value is approximately 1 order greater than the former value, which is probably caused by the difference in the wall structure at pH 10.4 and 3.4. At pH 10.4, the wall is in a shrunken state and the PS layers are intact; thus the diffusion of water would be as difficult as diffusion through pure polystyrene films of comparable thickness. In fact, the diffusion value, 3×10^{-13} $cm^2 \cdot s^{-1}$, is close to that obtained for a thin polystyrene film ($\sim 2.5 \times 10^{-13}$ $cm^2 \cdot s^{-1}$).[77] At pH 3.4, the wall is in a swollen state and the PS layers are cracked; thus the diffusion of water out of vesicles would be easier. One might expect that the diffusion coefficient at pH 3.4 would be much greater than that obtained from polystyrene films, because the intermediate component of the wall, the PDEA layer, is a hydrogel. It has to be pointed out that the rate-determining parts of the barrier during the water diffusion are the two polystyrene layers. During vesicle size decrease, once the outer PS layer cracks to release the swelling pressure from the intermediate PDEA layer, the inner PS layer cracks much less extensively, as seen in cryo-TEM images at pH 3.4 (see Figure S12 in the Supporting Information). In this case, the diffusion of water through the inner PS layer becomes the rate-determining step during the diffusion process, and the overall diffusion coefficient at low pH is not as high as might be anticipated.

7. Diffusion of Protons across Vesicle Wall. It was also of interest to investigate the diffusion of protons through the walls of the vesicles. Different HCl solutions are used to carry out the proton diffusion experiment with the help of a pH-sensitive water-soluble fluorescent dye, 8-hydroxypyrene-1,3,6-trisulfonic acid trisodium salt (shortened to HPTS), which cannot diffuse through the membrane. Specifically, the HPTS was encapsulated into the vesicle interior while the external HPTS in the solution was removed by ion-exchange. Thus, HPTS is present only in the vesicle interior. The diffusion experiment was performed

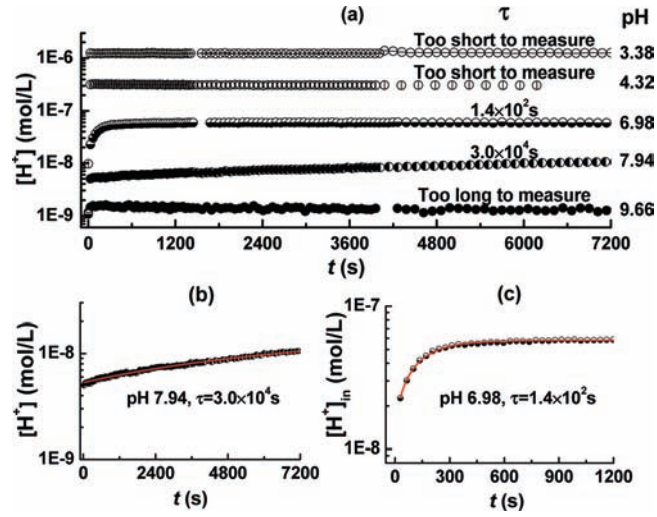

Figure 8. Internal proton concentration $[H^+]_{in}$ changes upon the addition of HCl. (a) Results for pH 3.38−9.66; (b and c) enlarged plots of the diffusion process at pH 7.94 and 6.98, respectively. The vesicles were prepared at pH 10.4 with a pH-sensitive water-soluble fluorescent dye HPTS present only in the vesicle interior. The external solution pH after equilibration was measured by pH meter.

by first adding a small amount of HCl into the external vesicle solution; then the pH-dependent excitation spectra of the HPTS were recorded. The results are shown in Figure 8 with the internal proton concentration, $[H^+]_{in}$, as determined from the shape of the spectra (see Figures S3, S4 in the Supporting Information), plotted as a function of time. The final solution pH, measured by a pH meter, can be regarded as the pH immediately after the HCl addition due to the negligible total interior vesicle volume relative to the total solution volume (<0.1%) (see Supporting Information for details).

It is clear from the shapes of the curves in Figure 8 that at different pH values the internal proton concentration $[H^+]_{in}$ changes over three very different time scales. When the initial pH is relatively high, e.g., 9.66, essentially no $[H^+]_{in}$ changes are observed within an experimental time of 2 h; when the initial pH increases to 7.94, significant $[H^+]_{in}$ changes are seen in

(77) Hong, P. P.; Boerio, F. J.; Clarson, S. J.; Smith, S. D. *Macromolecules* **1991**, *24*, 4770–4776.

Figure 8a and the enlarged plot in Figure 8b. When the initial pH is raised to 6.98, a typical exponential curve is observed in Figures 8a and 8c. Finally, when the initial pH is further increased to 4.32 or 3.38, again no $[H^+]_{in}$ changes can be seen as a function of time, but only a burst increase of $[H^+]_{in}$ immediately after the addition of the HCl. From the $[H^+]_{in}$ versus time profiles for pH 7.94 and 6.98, the apparent diffusion coefficient D of protons across the vesicle wall can be calculated to be 5.6×10^{-16} and 1.5×10^{-13} $cm^2 \cdot s^{-1}$. In the absence of the partition coefficient (protons in water versus protons in the wall), a direct comparison with other reported values is impossible; however, an apparent increase of D, as pH decreases, can still be seen. For processes at pH 4.32 and 3.38, it seems that protons diffuse into the vesicle interior immediately upon the addition of HCl, so the diffusion coefficient D at low pH is too high to be measured by the techniques used here. By contrast, for pH 9.66, diffusion is too slow to be measured. The diffusion results presented here clearly show that, as expected, the vesicle wall in its swollen state (low pH) is much more permeable than in its shrunken state (high pH).

The increase of the apparent diffusion coefficient D from too low to be measured at pH 9.66 to 5.6×10^{-16} $cm^2 \cdot s^{-1}$ at pH 7.94 and 1.5×10^{-13} $cm^2 \cdot s^{-1}$ at pH 6.98 to a value too high to be measured at pH 3.38 is, again, undoubtedly related to the wall structure at different pH values. At high pH, both the PS layers and the PDEA layer are hydrophobic; thus the diffusion of polar species, such as protons, will be difficult. As pH decreases, the intermediate PDEA layer starts swelling, so only the inner and outer PS layers are the major barriers for proton diffusion; the diffusion coefficient D increases. When the pH further decreases to below 6.0, neither the cracked PS layers nor the swollen PDEA layer are major barriers for proton diffusion; thus very fast diffusion is observed. The schematic illustrations for proton diffusion in these cases are shown in the Supporting Information.

Conclusion

A vesicle system with a pH-induced "breathing" feature and consisting of a three-layered wall structure is described. The "breathing" feature consists of a highly reversible vesicle size change accompanied by diffusion of species into and out of the vesicles. The "breathing" feature can be repeated many times, with a relaxation time of ca. 1 min.

The triblock copolymer PEO_{45}-b-PS_{130}-b-$PDEA_{120}$ was synthesized via ATRP and allowed to self-assemble into vesicles at pH 10.4. The vesicle wall was shown by cryo-TEM to consist of a sandwich of two ca. 4 nm thick PS layers and one ca.17 nm thick PDEA layer in the middle; the present system is thus different from the monolayer or bilayer structures reported previously for vesicles. As the pH decreases, the vesicle size increases, accompanied by an increase in the thickness of all three layers. The increase of the thickness of the intermediate PDEA layer arises from the protonation and hydration, but the swelling is constrained by the PS layers, which may be rubber-like because of their thinness. The increase of the thickness of the two PS layers with decreasing pH is a result of an increasing incompatibility and an accompanying sharpening of the interface between the PS layers and the PDEA layer. At a pH slightly below 6, progressive swelling of the PDEA layer induces cracks in the two PS layers, at which point both the wall thickness and the vesicle size show a sharp increase due to the now less constrained swelling of the intermediate PDEA layer. At pH 3.4, these changes reach a steady state: the vesicle wall shows a cracked surface, and the vesicle size has increased by 190%. These changes occurring between pH 10.4 and 3.4 are highly reversible and can be cycled repeatedly.

In the swollen state, the vesicles are highly permeable to water molecules (diffusion coefficient $D \approx 3 \times 10^{-12}$ $cm^2 \cdot s^{-1}$). In addition, the vesicle wall shows a pH-dependent permeability to protons, from essentially zero diffusion at high pH, to a dramatically increased diffusion with decreasing pH ($D \approx 5.6 \times 10^{-16}$ $cm^2 \cdot s^{-1}$ at pH 7.94 and 1.5×10^{-13} $cm^2 \cdot s^{-1}$ at pH 6.98, respectively), and finally to extremely fast diffusion at low pH.

Acknowledgment. It is of great pleasure for A.E. and S.Y. to acknowledge financial support from NSERC Canada (grant number RGPIN 4565-04) and for IR funding from CIHR (grant number MOP-86693) as well as the receipt of a CIHR New Investigator award.

Supporting Information Available: The entire experimental section, which also deals with the determination of pH of the vesicle interior; also provided are all of the calculations mentioned in the paper and more (cryo-)TEM images among others. This information is available free of charge via the Internet at http://pubs.acs.org.

JA902869Q